Elevated Cerebral Blood Flow and Volume in Systemic Lupus Measured by Dynamic Susceptibility Contrast Magnetic Resonance Imaging

CHARLES M. GASPAROVIC, CARLOS A. ROLDAN, WILMER L. SIBBITT Jr, CLIFFORD R. QUALLS, PAUL G. MULLINS, JANEEN M. SHARRAR, J. JEREMY YAMAMOTO, and H. JEREMY BOCKHOLT

ABSTRACT. ***Objective.*** Studies that have examined abnormalities in cerebral blood flow (CBF) in patients with systemic lupus erythematosus (SLE) reported CBF relative to a region assumed to be normal in the brain. We examined the absolute differences in both regional CBF and cerebral blood volume (CBV) between patients with SLE and healthy controls.

Methods. CBF and CBV were measured with dynamic susceptibility contrast (DSC) magnetic resonance imaging (MRI), a technique that provides an alternative to radionuclide perfusion studies and permits quantitative anatomic, CBF, and CBV imaging in a single scanning session. CBF and CBV were measured in lesions and in normal-appearing tissue in the major cerebral and subcortical brain regions. Unlike most perfusion studies in SLE, CBF and CBV values were not normalized to a region of the brain assumed to be healthy.

Results. CBF and CBV within MRI-visible lesions were markedly reduced relative to surrounding normal-appearing white matter. CBF and CBV in normal-appearing tissue were both higher in SLE patient groups, with or without lesions, relative to the control group.

Conclusion. DSC MRI, without normalization to a region presumed to be healthy, revealed that CBF and CBV in normal-appearing tissue in patients with SLE was higher than CBF and CBV in controls. Since this finding was made in subgroups of patients with and without lesions, the higher CBF and CBV appear to precede lesion pathology. (First Release June 15 2010; J Rheumatol 2010; 37:1834–43; doi:10.3899/jrheum.091276)

Key Indexing Terms:
LUPUS BRAIN CEREBRAL BLOOD FLOW
CEREBRAL BLOOD VOLUME MAGNETIC RESONANCE IMAGING

Systemic lupus erythematosus (SLE) can produce a wide variety of neurologic and psychiatric syndromes, including headache, chorea, cognitive dysfunction, and psychosis[1]. Histopathologic studies have shown evidence of widespread parenchymal and cerebrovascular injury, including thromboembolic vasculopathy, infarction, gliosis, and diffuse neuronal and axonal loss with varying degrees of inflammation[2]. Evidence of brain injury and altered brain physiology in SLE also comes from studies on neurometabolism measured by ^{18}F fluorodeoxyglucose (^{18}FDG) positron emission tomography (PET) or magnetic resonance spectroscopy[3,4,5,6,7,8], and radionuclide cerebral blood flow (CBF) studies[3,8,9,10,11,12,13,14,15,16,17,18,19,20,21], the majority based on single photon emission computed tomography (SPECT). Diffuse patchy areas of regionally reduced perfusion have been reported in diffuse neuropsychiatric SLE (NPSLE) syndromes, while focal areas of regionally reduced perfusion may occur in focal NPSLE[13,16,17,18]. These abnormalities may be conspicuous in presumed areas of neurologic impairment and improve with corticosteroid therapy or clinical resolution[15,19]. However, at least 1 study examining SLE subjects with and without neuropyschiatric symptoms reported no relationship between NPSLE, neurocognitive function, and perfusion abnormalities, suggesting that reduced perfusion may not be a hallmark of NPSLE[11].

In contrast to the many SPECT studies on SLE, far fewer studies have examined CBF using perfusion methods based

From the Department of Psychology, Divisions of Cardiology and Rheumatology, Department of Internal Medicine, School of Medicine, University of New Mexico, Albuquerque; The Mind Research Network, Albuquerque, New Mexico, USA; and the Bangor Imaging Center, School of Psychology, Bangor University, Gwynedd, UK.

Supported by grants RO1 HLO77422-01-A3 and M01 RR00997 from the National Institutes of Health.

C. Gasparovic, PhD, Department of Psychology, School of Medicine, University of New Mexico, The Mind Research Network; H.J. Bockholt, BS, The Mind Research Network; C. Qualls, PhD, Department of Internal Medicine, School of Medicine, University of New Mexico; P.G. Mullins, PhD, Bangor Imaging Center, School of Psychology, Bangor University; J. Sharrar, BSN, Department of Internal Medicine, School of Medicine, University of New Mexico; J. Yamamoto, MS, The Mind Research Network; W.L. Sibbitt Jr, MD; C.A. Roldan, MD, Department of Internal Medicine, School of Medicine, University of New Mexico.

Address correspondence to C. Gasparovic, Pete and Nancy Domenici Hall, University of New Mexico, 1101 Yale Blvd. NE, Albuquerque, NM 87106, USA. E-mail: chuck@unm.edu

Accepted for publication April 1, 2010.

on PET or magnetic resonance imaging (MRI). PET, while costly and exposing the patient to high-energy ionizing radiation, is considered one of the most accurate methods for CBF measurement[22]. A less costly alternative approach is dynamic susceptibility contrast (DSC) MRI[23], which can be conveniently performed in the same examination as anatomic MRI, is inherently coregistered to the anatomical images, and most important, does not expose the patient or examiner to ionizing radiation or radionuclides. While 2 early studies using PET found evidence of transient reduced[21] or lower CBF in a single subject[20], a more recent PET study found higher CBF relative to control subjects in anemic, hypertensive patients with chronic renal failure, including 1 patient with SLE[24]. Only 1 study on SLE using DSC MRI has been reported[25]. In that study, both SPECT and DSC MRI were applied and revealed areas of relative hypoperfusion in SLE subjects, with SPECT detecting more hypoperfused areas than DSC MRI. However, CBF differences in these studies were evaluated qualitatively or normalized relative to CBF in a region of the brain presumed to be unaffected by disease. To our knowledge, absolute regional differences in CBF between SLE and control subjects have not been reported. Further, quantitative cerebral blood volume (CBV) abnormalities in SLE, not measureable by conventional SPECT, have yet to be reported.

The purpose of our study was to use DSC MRI to quantitatively measure both cerebral perfusion and blood volume in patients with SLE and healthy controls using non-normalized measures of CBF and CBV. Segmentation of the anatomical images acquired in the same scanning session as the DSC MRI images allowed calculation of mean gray and white matter CBV and CBF values in cerebral (occipital, parietal, temporal, and frontal) and subcortical (caudate, putamen, thalamus, and globus pallidus) regions and within brain lesions for both patients and controls.

MATERIALS AND METHODS

Subjects. Forty-two SLE subjects and 19 age- and sex-matched healthy controls were studied. The diagnosis of SLE was established in each subject using the American College of Rheumatology (ACR) 1997 revised criteria[26]. SLE disease activity was determined with the SLE Disease Activity Index (SLEDAI), SLE-associated injury was measured with the Systemic Lupus International Collaborating Clinics (SLICC)/ACRDI (damage index), and NPSLE activity was determined with the neurologic subsets of both neuro-SLEDAI and neuro-SLICC/ACRDI as reported[27]. Past and present neuropsychiatric symptoms and findings were classified using the 1999 ACR Case Definitions for NPSLE[28]. Important demographic features of the SLE group are shown in Table 1.

The study was approved by the University of New Mexico Institutional Review Board and conformed to the Declaration of Helsinki. All subjects provided informed consent and signed formal permission for all procedures.

MRI. Anatomical MRI, DSC MRI, and MR angiography were performed on all subjects using a 1.5-Tesla Siemens Sonata scanner with an 8-channel head coil. The total time of the MRI protocol was about 1 hour. Scout images were used to prescribe a series of whole-head T1-weighted, T2-weighted, and fluid attenuated inversion recovery (FLAIR) images aligned with the interhemispheric midline and parallel to the anterior commissure-posterior commissure (AC-PC) line. T1-weighted images [3D fast low angle shot (FLASH) sequence, TR/TE 12/4.76 ms, flip angle 20°, field of view (FOV) 256 × 256 mm, resolution 1 mm × 1 mm, 128 slices, slice thickness 1.5 mm] and T2-weighted images (turbo spin-echo sequence, TR/TE 9040/64 ms, turbo factor 5, FOV 220 × 220 mm, resolution 1.1 × 1.1 mm, 128 slices, slice thickness 1.5 mm) were acquired for anatomical segmentation of normal-appearing gray matter (GM), white matter (WM), and cerebrospinal fluid (CSF). The FLAIR image (variable flip, TR/TE/TI 6000/358/2100 ms, averages 2, slice thickness 1.5 mm, FOV 220 mm, matrix size 192 × 192) was used to manually segment lesions. The segmented GM, WM, CSF, and lesion maps were used to identify these regions in the processed perfusion maps. The DSC MRI images were acquired with a perfusion-weighted echo planar imaging (EPI) sequence (TR 1430 ms/TE 46 ms/flip 90°, 20 slices, time course of 50 sequential acquisitions, FOV 200 mm^2, matrix 128 × 128). Gadopentetate dimeglumine contrast agent (Magnevist®; Bayer HealthCare Pharmaceuticals, www.bayerus.com) was injected into an antecubital vein at the standard dose (0.1 ml/kg body weight) using a power injector at 5 ml/s, starting 15 s after the start of scan acquisition, followed by 20 ml saline at the same rate. The central volume principle allows perfusion characteristics (blood flow and volume) to be estimated from the signal profile generated by the contrast bolus[23]. Raw DSC MRI data were analyzed using the Penguin software package (NordicImagingLab, Bergen, Norway). The software converts pixel intensity changes due to contrast (gadopentetate) passage over the time series of images into pixel by pixel tissue contrast concentration curves, C(t). With user supervision, it selects candidate arterial pixels to construct an arterial input function, AIF(t), based on the higher intensities and narrow time courses of the concentration changes. An attempt was made to locate and use pixels associated with the middle cerebral artery consistently for the construction of the AIF(t). A gamma variate function is fit to the raw C(t) and AIF(t) curves to identify just the first pass of the contrast bolus and is used to represent C(t) and AIF(t) in further analyses. The CBV in any pixel is calculated as the ratio of areas under the tissue and artery concentration curves $K \times \int C(t)\,dt / \int AIF(t)\,dt$. The constant K was set to 1 rather than to a value based on assumed capillary and artery hematocrits and tissue density[29]. The calculation of CBF is more complex, and involves an equation relating C(t) to CBF and the convolution of AIF(t) and the residue function R(t), the fraction of contrast agent in the vasculature at any time: $C(t) = K \times CBF \times [AIF(t) \otimes R(t)]$, where $\otimes$ denotes the convolution operator. Various strategies have been proposed for deconvolving AIF(t) from R(t) in order to solve this equation for CBF[23]. We applied the circular singular value decomposition method[30] available as an option in Penguin that has been shown to provide robust CBF measures in the presence of variable delays between bolus arrival in the arterial pixels defining the AIF(t) and the tissue pixels defining C(t). The CBV and CBF maps constructed with Penguin were coregistered to the T1-weighted images to identify distinct brain regions within gray and white matter. This procedure involved automatically segmenting the T1-weighted image into GM, WM, and CSF and coregistering the lesion map that was manually traced from the FLAIR image to the T1-weighted image. The T1-weighted image was warped into a standard brain template for identifying the major cortical and subcortical brain regions. Finally, the resulting regionally segmented map was transformed back into the native space of the CBV and CBF maps. These steps were accomplished with the BRAINS2 software[31]. GM and WM values for 4 cerebral regions (occipital, parietal, temporal, and frontal) and 4 subcortical regions (caudate, putamen, thalamus, and globus pallidus) for each hemisphere are reported. These regions of interest are shown in a representative T1-weighted image from one subject in Figure 1. Mean CBV and CBF values in lesions are also reported. In order to resolve CBV and CBF in normal-appearing tissue from CBV and CBF in lesions, the mean regional cerebral or subcortical values of CBV and CBF reported were calculated without the lesion pixels included. This allowed us to observe similarities in normal-appearing tissue between lupus groups (those with and those without lesions) without the confound of the lower lesion CBV and CBF values reducing the overall mean values for the region.

Table 1. Demographic data and clinical assessments of the SLE subjects.

Characteristic	SLE with Lesions, n = 23	SLE without Lesions, n = 19	p
Age, yrs	41.5 ± 11.7	34.0 ± 12.3	0.051
Female, %	91.3	94.7	0.66*
Age at onset of SLE, yrs	31.4 ± 11.1	26.2 ± 14.6	0.21
Disease duration, yrs	11.0 ± 8.0	7.5 ± 5.7	0.11
Prednisone, mg/day	13.0 + 41.4	5.8 ± 11.3	0.43
Hydroxychloroquine, %	47.8	47.4	0.99*
Cyclophosphamide, %	26.1	36.8	0.52*
Mycophenolate, %	17.4	10.5	0.67*
SLEDAI, U	11.9 ± 10.5	10.2 ± 7.7	0.55
SLICC-ACR/DAI, U	3.7 ± 2.5	3.1 ± 2.3	0.39
Neuro-SLEDAI, U	4.5 ± 6.7	2.1 ± 4.5	0.17
Neuro-SLICC, U	1.2 ± 1.3	0.6 ± 0.9	0.08
Antinuclear antibody titer	294 ± 396	360 ± 463	0.62
Anti-dsDNA antibody titer	14.9 ± 36.9	54.0 ± 59.8	0.02
C3, mg/dl	104 ± 36	100 ± 30	0.70
C4, mg/dl	25 ± 35	16 ± 7	0.27
Erythrocyte sedimentation rate, mm/h	29 ± 34	20 ± 14	0.24
C-reactive protein, mg/dl	1.2 ± 1.7	1.1 ± 1.5	0.75
aPL IgG, IU	10.7 ± 10.5	18.2 ± 27.1	0.26
aPL IgM, IU	12.0 ± 17.7	10.0 ± 14.3	0.70
aPL IgA, IU	6.5 ± 12.8	6.4 ± 11.9	0.99
Lupus-like inhibitor, %	27.3	42.1	0.35*
Antiribosomal P antibody (dilutions)	1.5 ± 3.0	10.8 ± 32.4	0.24

* Satterthwaite's t-test was used except for binary data where Fisher's exact test was used.

Statistical analysis. Group differences in regional CBV and CBF among SLE subgroups (with and without lesions) and the controls were analyzed by repeated measures (RM) ANOVA with the 3 groups as the grouping factor and the different brain regions as a repeated factor. This approach was motivated by the fact that CBF and CBV are known to vary from region to region in the brain and hence, statistical comparisons based on CBF or CBV averaged over the whole brain will fail to identify differences in the regional variation of these measurements. RM ANOVA was performed in each of 3 general tissue types: cerebral gray matter, cerebral white matter, and subcortical gray matter. Posthoc pairwise comparisons were made using Wald's t-test. The RM model in each general region was constructed with brain hemisphere and specific region (e.g., occipital, parietal, temporal, and frontal) as repeated factors (e.g., see Table 2). Correlations between CBF and antiphospholipid antibody (aPL) tests were examined with linear regression and Spearman's rank correlation coefficient. All statistical analyses were performed with SAS® (http://www.sas.com).

RESULTS

Forty-two SLE subjects and 19 controls were studied. The SLE and control groups were similar in age (SLE 38.1 ± 12.4 yrs, controls 34.8 ± 11.9 yrs; p = 0.33), sex (SLE 95% women, controls 89%; p = 0.58), weight (SLE 71.4 ± 14.0 kg, controls 69.7 ± 11.9 kg; p = 0.63), and body mass index (SLE 26.65 ± 4.7 kg, controls 25.8 ± 5.0 kg; p = 0.56). Twenty-three (54.8%) SLE subjects had focal lesions that were detectable on FLAIR images. As expected, the total lesion volume in the group of patients with SLE varied, with a median of 0.70 cm^3 and interquartile range 0.21 to 5.99 cm^3. However, regression analysis revealed no significant correlation between lesion volume and CBF or CBV in nonlesion tissue in these subjects. Among patients without hypertension (systolic blood pressure < 140 mm Hg, diastolic < 90 mm Hg), 48% (16/33) had lesions and among those with hypertension, 88% (7/8) had lesions. Using Fisher's exact test, the correlation between the presence of lesion and hypertension was found not to be significant. Subjects with lesions tended to be older (p = 0.051) and to have lower levels of anti-dsDNA antibodies (p = 0.02) than those without lesions. However, subjects with and without lesions were very similar in all other clinical and laboratory measures, including anticardiolipin antibodies and lupus-like inhibitor, SLE disease activity (SLEDAI), SLE damage (SLICC-ACRDI), NPSLE activity (Neuro-SLEDAI), and damage caused by NPSLE (Neuro-SLICC; Table 1). The lesions were located almost exclusively in white matter regions and predominantly in the frontal and parietal lobes. Anatomical and perfusion images from one subject are shown in Figure 1, demonstrating a pronounced reduction in perfusion at the site of a lesion evident in the FLAIR image. A significant group difference in aPL levels between SLE groups with and without lesions was not observed in this sample.

A regional pattern of posterior to anterior increase in CBF was observed in all groups (Figure 2), in agreement with perfusion studies using other methods[32,33] and reflected by a similar pattern of CBV across the brain (Figure 2). Thus, occipital and parietal lobes were consistently less perfused than the frontal lobes and, within subcortical regions, the globus pallidus was less perfused than the caudate nucle-

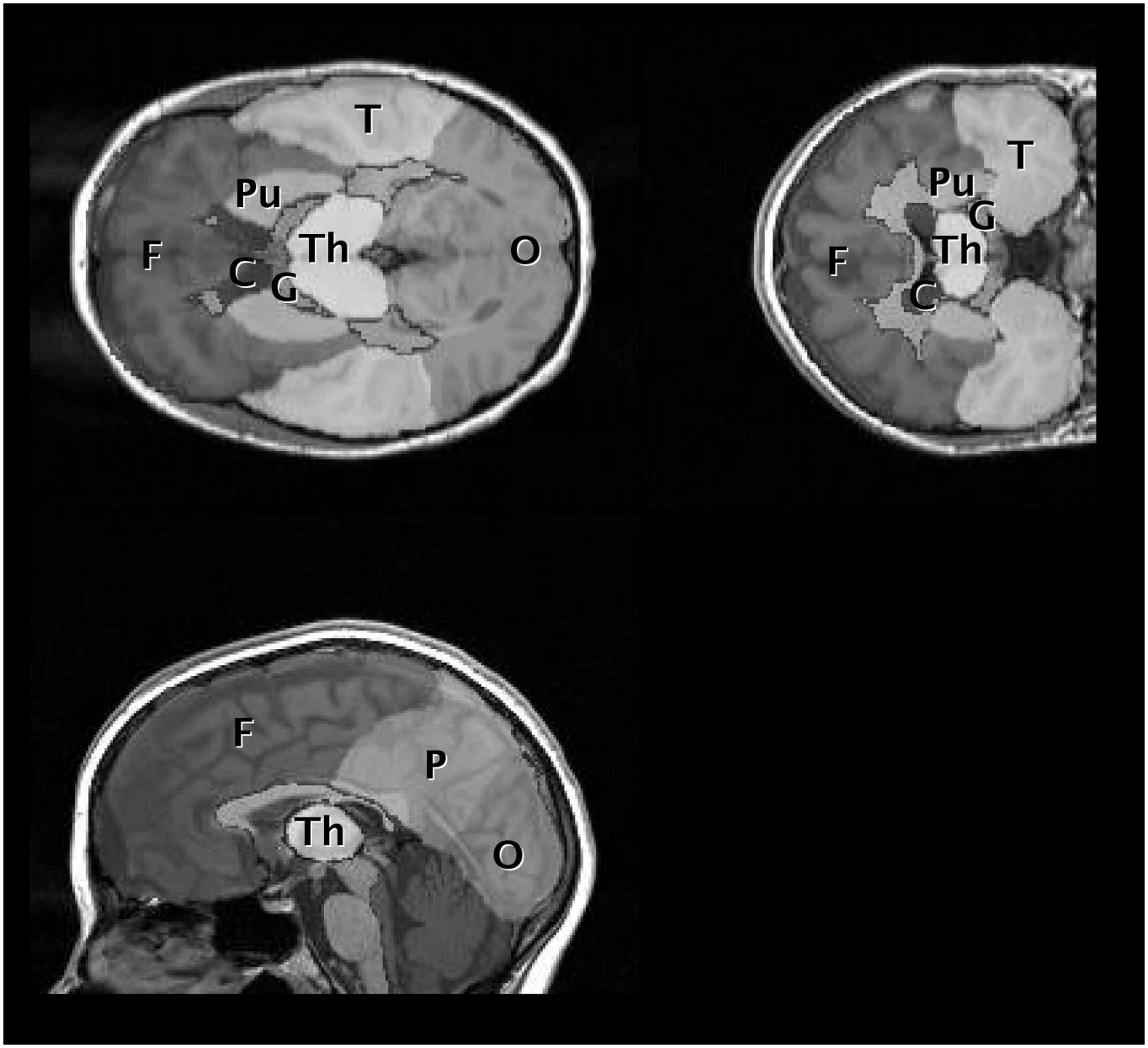

Figure 1. T1-weighted image from one control patient with regions of interest overlaid. F: frontal, P: parietal, T: temporal, O: occipital, G: globus pallidus, C: caudate, Pu: putamen, Th: thalamus.

us in all subject groups. Also, as expected, both CBF and CBV in MRI-visible lesions were significantly reduced ($p < 0.001$) relative to normal-appearing white matter (Tables 2 and 3), indicating a disruption of vascular-parenchymal integrity in MR-visible lesions. Finally, both CBF and CBV were higher in the SLE groups (with or without lesions) relative to the control group (Tables 2 and 3). RM ANOVA and posthoc pairwise t-tests, used to examine group differences across either all cerebral gray matter, all cerebral white matter, or all subcortical gray matter regions, revealed that both CBV and CBF were significantly higher in SLE subjects than in controls in all regions except possibly in subcortical gray matter for CBF, where the p value was 0.051. Neither prednisone use nor multiple measures of disease activity (i.e., SLEDAI, Neuro-SLEDAI, SLICC, Neuro-SLICC) correlated significantly with CBF or CBV. A trend to higher CBV and CBF in SLE subjects without MRI-detectable lesions relative to those with lesions was also observed, indicating that the underlying cause of elevated blood volume and perfusion in SLE subjects may be independent of MR-visible lesions and may precede MRI-detectable lesion formation.

Table 2. Regional mean cerebral blood flow (CBF) values (ml/min/100 g tissue) in SLE subjects with and without lesions and healthy controls. Repeated measures (RM) ANOVA results are given for the main effects of group, hemisphere, and region for each tissue class (cerebral gray matter, white matter, subcortical gray).

Region	Group			RM ANOVA	
	Control, mean (SD)	SLE without Lesions, mean (SD)	SLE with Lesions, mean (SD)	Main Effect	p
Cerebral gray matter				Group	0.007
Left hemisphere				Hemisphere	0.399
Frontal	20.0 (5.9)	22.3 (7.5)	20.7 (5.4)	Region	0.353
Parietal	20.7 (5.5)	23.4 (8.4)	21.4 (5.7)		
Temporal	21.4 (5.4)	23.0 (6.9)	22.2 (4.8)		
Occipital	21.3 (6.3)	24.7 (8.2)	22.0 (5.8)		
Right hemisphere					
Frontal	19.8 (5.2)	22.4 (7.3)	20.3 (4.8)		
Parietal	20.5 (5.7)	22.4 (8.5)	21.7 (5.4)		
Temporal	21.5 (5.4)	23.4 (7.0)	22.4 (4.7)		
Occipital	19.7 (5.9)	21.6 (7.5)	21.5 (5.3)		
Cerebral white matter				Group	< 0.001
Left hemisphere				Hemisphere	0.800
Frontal	13.2 (4.3)	14.9 (5.4)	14.8 (4.1)	Region	< 0.001
Parietal	14.2 (4.3)	17.2 (7.1)	15.5 (4.0)		
Temporal	16.0 (5.4)	18.5 (6.5)	17.8 (4.2)		
Occipital	18.1 (5.8)	21.8 (7.3)	18.6 (5.4)		
Right hemisphere					
Frontal	13.3 (3.8)	14.8 (5.4)	14.9 (3.9)		
Parietal	14.8 (4.9)	17.1 (6.4)	16.2 (4.3)		
Temporal	17.1 (5.5)	19.5 (6.8)	18.7 (4.5)		
Occipital	17.2 (5.5)	19.7 (7.5)	18.7 (4.9)		
Subcortial				Group	0.051
Left hemisphere				Hemisphere	0.471
Globus pallidus	14.1 (5.0)	16.0 (8.6)	13.3 (5.4)	Region	< 0.001
Caudate	14.9 (6.4)	16.4 (10.0)	13.7 (7.7)		
Putamen	16.3 (4.9)	18.4 (7.7)	16.3 (6.7)		
Thalamus	18.6 (7.3)	21.9 (8.5)	21.6 (6.7)		
Right hemisphere					
Globus pallidus	13.0 (4.5)	15.6 (7.2)	14.2 (5.7)		
Caudate	13.5 (4.7)	15.8 (8.8)	14.4 (7.4)		
Putamen	15.9 (5.1)	17.1 (7.2)	16.6 (6.2)		
Thalamus	19.6 (7.3)	19.8 (7.9)	20.1 (7.2)		
Lesion			9.7 (4.4)		< 0.001†

† Student t-test comparing mean lesion CBF and mean white matter CBF in each SLE subject.

DISCUSSION

Studies have found evidence of abnormal cerebral perfusion in patients with SLE[3,8,9,10,11,12,13,14,15,16,17,18,19,20,21]. The majority of these were based on SPECT methods and reported regional deficits in CBF relative to brain regions presumed to be normal within the individual subject. Using quantitative DSC MRI without normalization, we found that CBF was significantly reduced within MRI-visible brain lesions in patients with SLE, indicating a disruption of vascular-parenchymal integrity consistent with prior SPECT studies. However, our results indicate that both CBV and CBF were consistently higher in normal-appearing tissue in patients with SLE than in corresponding tissues in age- and sex-matched healthy controls (Figure 3, Tables 2 and 3). Additionally, no significant group differences in CBV or CBF between SLE subjects with lesions and those without lesions were observed, indicating that the causal factor or factors contributing to elevated cerebral perfusion were not directly related to and may not be caused by lesion load.

The CBF group differences demonstrating increased CBF in SLE that we observed are not necessarily in disagreement with previous findings of relative regional reductions in CBF in SLE patients, including at least 1 study comparing SPECT findings to DSC MRI findings[25]. The group differences in CBF in normal-appearing tissue observed in our study, based on non-normalized measures of CBV and CBF, would have been obscured by normalization to any particular region, since CBV and CBF in all brain regions in the SLE group were found to be elevated relative to those in the control group. As well, the precise coregistration of perfusion and lesion maps inherent in integrated anatomic-perfusion MRI allowed us to exclude lesions from the analysis

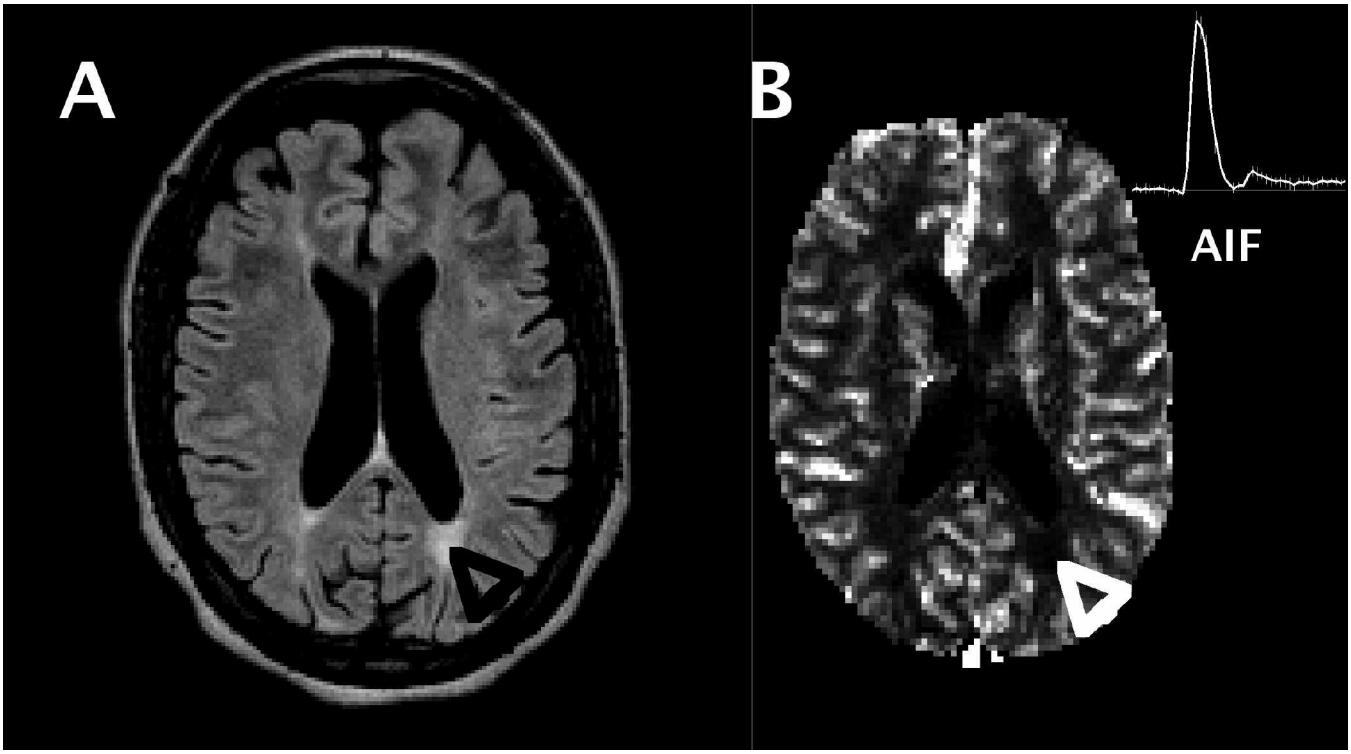

Figure 2. A. FLAIR image from one patient with SLE, with a white matter lesion indicated by black arrow (lower right quadrant of image). B. Cerebral blood flow (CBF) map from same subject showing reduced CBF in region of lesion (white arrow) and arterial input function (AIF) time course (upper right corner).

of normal-appearing tissue regions. Hence, the use of analysis methods in prior studies that normalized CBF by values in other brain regions and did not exclude obvious anatomic abnormalities could account for the absence of findings similar to those reported here. Finally, to our knowledge, this is the first report of direct comparisons of quantitative CBV between SLE and control groups. While issues concerning the accuracy of either MRI and SPECT-based perfusion measurements relative to PET are well known[22,34], the measurement of CBV by DSC MRI is more straightforward than the calculation of CBF, and derived simply from the ratio of the time courses of the arterial and tissue bolus concentration curves. The CBV group differences we observed closely paralleled the CBF group differences.

Cerebral hyperperfusion in SLE has been reported previously, but only in the basal ganglia of patients with SLE who have Parkinsonian syndrome, using relative measures of perfusion with SPECT[35,36]. However, in a study that included at least 1 patient with SLE, quantitative PET was used to observe higher CBF throughout the brain of patients with renal disease relative to healthy controls[24]. Hyperperfusion has also been reported in other neurological disorders, including stroke[37], occlusive sickle-cell disease[38], transient ischemic attack[39], seizures and epilepsy[40], traumatic brain injury[41], metabolic brain disease[42], and migraine[43]. Increased CBV can also be observed in the symptom-free interval of a transient ischemic attack, the acute state of a completed infarction, traumatic brain injury, nonenhancing lesions of multiple sclerosis, and normal-appearing tissue in multiple sclerosis[44]. The increased CBV reported in stroke may indicate intact vascular beds with potentially salvageable areas in the penumbra of the lesion[45]. Further, increases in CBV can be a sign of vasomotor instability, a compensatory mechanism indicating resolving injury, or a reduction of compensatory capacity in response to further ischemia or injury[46].

MRI is presently the preferred anatomic neuroimaging modality to evaluate NPSLE[47]. While $H_2{}^{15}O$ PET remains the "gold standard" for cerebral perfusion studies, it is costly, involves the use of a catheter to measure the arterial $H_2{}^{15}O$ concentration, involves high-energy ionizing radiation, and requires immediate proximity to a cyclotron that can generate the short-lived ^{15}O radioisotope. SPECT offers a practical alternative to PET, but may have limitations in accuracy relative to PET, and therefore is most commonly used to assess relative CBF differences rather than absolute quantitative measures of CBF[34]. While studies have demonstrated that SPECT and DSC MRI are comparable to each other in accuracy[48], DSC MRI has the advantages of not using radioisotopes, having higher spatial resolution, and allowing the measurement of CBV as well as CBF. The risks with the use of gadolinium-based contrast agents in DSC MRI are small and identical to those associated with the use of these agents for routine contrast MRI scans, but include an association with nephrogenic systemic fibrosis, possibly due to free gadolinium toxicity, in subjects with endstage

Table 3. Regional mean cerebral blood volume (CBV) values (ml/100 g tissue) in SLE subjects with and without lesions and healthy controls. Repeated measures (RM) ANOVA results are given for the main effects of group, hemisphere, and region for each tissue class (cerebral gray matter, white matter, subcortical gray).

Region	Group			RM ANOVA	
	Control, mean (SD)	SLE without Lesions, mean (SD)	SLE with Lesions, mean (SD)	Main Effect	p
Cerebral gray matter				Group	< 0.001
Left hemisphere				Hemisphere	0.481
Frontal	1.85 (0.42)	2.16 (0.63)	2.06 (0.46)	Region	0.290
Parietal	1.88 (0.49)	2.23 (0.74)	2.12 (0.55)		
Temporal	2.03 (0.44)	2.28 (0.64)	2.30 (0.47)		
Occipital	2.01 (0.54)	2.48 (0.95)	2.29 (0.61)		
Right hemisphere					
Frontal	1.83 (0.42)	2.18 (0.57)	2.04 (0.45)		
Parietal	1.88 (0.47)	2.15 (0.75)	2.19 (0.53)		
Temporal	2.06 (0.45)	2.34 (0.62)	2.31 (0.51)		
Occipital	1.86 (0.45)	2.12 (0.71)	2.24 (0.75)		
Cerebral white matter				Group	< 0.001
Left hemisphere				Hemisphere	0.887
Frontal	1.23 (0.30)	1.48 (0.48)	1.50 (0.41)	Region	< 0.001
Parietal	1.30 (0.34)	1.66 (0.64)	1.55 (0.36)		
Temporal	1.51 (0.40)	1.88 (0.66)	1.85 (0.43)		
Occipital	1.68 (0.49)	2.16 (0.84)	1.86 (0.57)		
Right hemisphere					
Frontal	1.25 (0.28)	1.45 (0.45)	1.50 (0.38)		
Parietal	1.37 (0.39)	1.66 (0.57)	1.62 (0.40)		
Temporal	1.64 (0.45)	1.93 (0.61)	1.93 (0.48)		
Occipital	1.58 (0.42)	1.90 (0.73)	1.89 (0.48)		
Subcortial				Group	0.015
Left hemisphere				Hemisphere	0.6894
Globus pallidus	1.18 (0.49)	1.54 (0.88)	1.15 (0.39)	Region	< 0.001
Caudate	1.52 (0.62)	1.58 (0.84)	1.48 (0.72)		
Putamen	1.35 (0.38)	1.66 (0.64)	1.47 (0.56)		
Thalamus	2.14 (1.09)	2.65 (1.25)	2.71 (1.02)		
Right hemisphere					
Globus pallidus	1.07 (0.31)	1.46 (0.72)	1.29 (0.49)		
Caudate	1.45 (0.47)	1.62 (0.77)	1.59 (0.78)		
Putamen	1.34 (0.44)	1.53 (0.62)	1.47 (0.49)		
Thalamus	2.31 (1.07)	2.34 (1.04)	2.58 (1.08)		
Lesion			1.00 (0.39)		< 0.001†

† Student t-test comparing mean lesion CBV and mean white matter CBV in each SLE subject.

renal disease[49]. Therefore, caution should be exercised in administering gadolinium-based contrast agents to subjects with highly compromised renal function.

Compared to non-MRI methods, DSC MRI allows easy and accurate registration of the CBF and CBV maps to MRI anatomical images acquired in the same scanning session. This latter advantage, for example, permitted accurate region-of-interest analysis of the CBF and CBV maps of this study in which mean CBF and CBV values were specifically assigned to gray matter, white matter, lesions, and the major anatomical regions after coregistration to high resolution T1-weighted and FLAIR images. This allowed us to observe not only the expected pattern of regional CBF and CBV differences within the brain, but also lower CBF and CBV in regions of small lesions. By not normalizing CBF and CBV values to values in a region presumed to be "normal," as has been done in most studies on SLE, we were able to observe differences between control and SLE groups. However, it is important to note that uncertainty in the arterial input function measurement (see Methods) has been shown to limit the accuracy of CBF and CBV values obtained with DSC MRI[50], hence the values reported here cannot be considered quantitative in the absolute sense. However, under the assumption that there was no systematic bias in the measurement of the AIF in either group, these values allow relative differences in both CBF and CBV between groups to be observed. Our findings, therefore, suggest that a similar approach of examining non-normalized CBF values, irrespective of the measurement method, be taken in future perfusion studies in SLE.

Our results demonstrate lower CBF and CBV in lesions but higher CBF and CBV throughout cortical and white

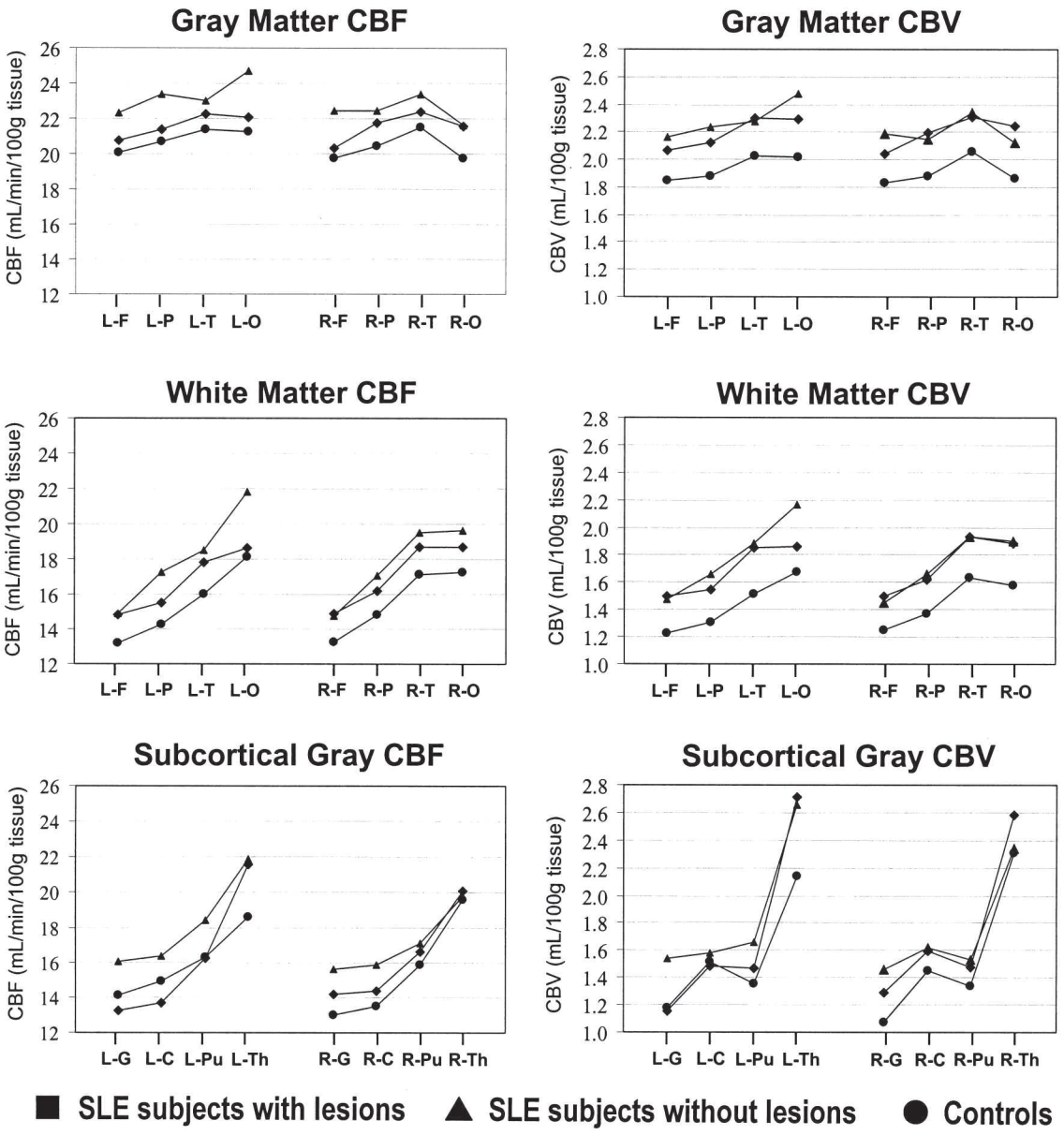

Figure 3. Plots of mean cerebral blood flow (CBF) and cerebral blood volume (CBV) values for each tissue class (gray matter, white matter, subcortical gray matter), hemisphere (left and right), and region (F: frontal, P: parietal, T: temporal, O: occipital, G: globus pallidus, C: caudate, Pu: putamen, Th: thalamus) in controls, SLE subjects with lesions, and SLE subjects without lesions.

matter regions of the brain in patients with SLE relative to controls. The higher global CBF and CBV values do not appear to be directly related to the presence of MRI-detectable lesions and may be due to other reactive physiologic or pathogenic factors underlying SLE, such as vasomotor instability, compensatory mechanisms for resolving injury, low-grade excitotoxicity due to antibody impairment of N-methyl D-aspartate (NMDA) receptors, or inflammatory factors[51]. Integrated DSC MRI and MRI is a robust method to measure CBF and CBV in specific anatomically defined tissues and may provide new insights into the neuropathology of SLE.

REFERENCES

1. Rhiannon JJ. Systemic lupus erythematosus involving the nervous system: presentation, pathogenesis, and management. Clin Rev Allergy Immunol 2008;34:356-60.
2. Jennekens FG, Kater L. The central nervous system in systemic lupus erythematosus. Part 1. Clinical syndromes: a literature investigation. Rheumatology 2002;41:605-18.
3. Grunwald F, Schomburg A, Badali A, Ruhlmann J, Pavics L, Biersack HJ. 18FDG PET and acetazolamide-enhanced 99m Tc-HMPAO SPET in systemic lupus erythematosus. Eur J Nucl Med 1995;22:1073-7.
4. Otte A, Weiner SM, Peter HH, Mueller-Brand J, Goetze M, Moser E, et al. Brain glucose utilization in systemic lupus erythematosus with neuropsychiatric symptoms: a controlled positron emission

tomography study. Eur J Nucl Med 1997;24:787-91.
5. Sibbitt WL Jr, Haseler LJ, Griffey RR, Friedman SD, Brooks WM. Neurometabolism of active neuropsychiatric lupus determined with proton MR spectroscopy. AJNR Am J Neuroradiol 1997;18:1271-7.
6. Weiner SM, Otte A, Schumacher M, Klein R, Gutfleisch J, Brink I, et al. Diagnosis and monitoring of central nervous system involvement in systemic lupus erythematosus: value of F-18 fluorodeoxyglucose PET. Ann Rheum Dis 2000;59:377-85.
7. Castellino G, Govoni M, Padovan M, Colamussi P, Borrelli M, Trotta F. Proton magnetic resonance spectroscopy may predict future brain lesions in SLE patients: a functional multi-imaging approach and follow up. Ann Rheum Dis 2005;64:1022-7.
8. Handa R, Sahota P, Kumar M, Jagannathan NR, Bal CS, Gulati M, et al. In vivo proton magnetic resonance spectroscopy (MRS) and single photon emission computerized tomography (SPECT) in systemic lupus erythematosus (SLE). Magn Reson Imaging 2003;21:1033-7.
9. Postiglione A, De Chiara S, Soricelli A, Oriente A, Ruocco A, Spadaro G, et al. Alterations of cerebral blood flow and antiphospholipid antibodies in patients with systemic lupus erythematosus. Int J Clin Lab Res 1998;28:34-8.
10. Huang JL, Yeh KW, You DL, Hsieh KH. Serial single photon emission computed tomography imaging in patients with cerebral lupus during acute exacerbation and after treatment. Pediatr Neurol 1997;17:44-8.
11. Waterloo K, Omdal R, Sjoholm H, Koldingsnes W, Jacobsen EA, Sundsfjord JA, et al. Neuropsychological dysfunction in systemic lupus erythematosus is not associated with changes in cerebral blood flow. J Neurol 2001;248:595-602.
12. Kobayashi H, Watanabe H, Seino T, Suzuki S, Sato Y. Quantitative imaging of cerebral blood flow using SPECT with 123I-iodoamphetamine in neuropsychiatric systemic lupus erythematosus. J Rheumatol 2003;30:2075-6.
13. Yoshida A, Shishido F, Kato K, Watanabe H, Seino O. Evaluation of cerebral perfusion in patients with neuropsychiatric systemic lupus erythematosus using 123I-IMP SPECT. Ann Nucl Med 2007;21:151-8.
14. Colamussi P, Trotta F, Ricci R, Cittanti C, Govoni M, Barbarella G, et al. Brain perfusion SPET and proton magnetic resonance spectroscopy in the evaluation of two systemic lupus erythematosus patients with mild neuropsychiatric manifestations. Nucl Med Commun 1997;18:269-73.
15. Emmi L, Bramati M, De Cristofaro MT, Mascalchi M, Dal Pozzo G, Marconi GP, et al. MRI and SPECT investigations of the CNS in SLE patients. Clin Exp Rheumatol 1993;11:13-20.
16. Kovacs JA, Urowitz MB, Gladman DD, Zeman R. The use of single photon emission computerized tomography in neuropsychiatric SLE: a pilot study. J Rheumatol 1995;22:1247-53.
17. Lin WY, Wang SJ, Yen TC, Lan JL. Technetium-99m-HMPAO brain SPECT in systemic lupus erythematosus with CNS involvement. J Nucl Med 1997;38:1112-5.
18. Russo R, Gilday D, Laxer RM, Eddy A, Silverman ED. Single photon emission computed tomography scanning in childhood systemic lupus erythematosus. J Rheumatol 1998;25:576-82.
19. Sun SS, Huang WS, Chen JJ, Chang CP, Kao CH, Wang JJ. Evaluation of the effects of methylprednisolone pulse therapy in patients with systemic lupus erythematosus with brain involvement by Tc-99m HMPAO brain SPECT. Eur Radiol 2004;14:1311-5.
20. Pinching AJ, Travers RL, Hughes GR, Jones T, Moss S. Oxygen-15 brain scanning for detection of cerebral involvement in systemic lupus erythematosus. Lancet 1978;1:898-900.
21. Volkow ND, Warner N, McIntyre R, Valentine A, Kulkarni M, Mullani N, et al. Cerebral involvement in systemic lupus erythematosus. Am J Physiol Imaging 1988;3:91-8.
22. Latchaw RE, Yonas H, Hunter GJ, Yuh WT, Ueda T, Sorensen AG, et al. Guidelines and recommendations for perfusion imaging in cerebral ischemia: A scientific statement for healthcare professionals by the writing group on perfusion imaging, from the Council on Cardiovascular Radiology of the American Heart Association. Stroke 2003;34:1084-104.
23. Ostergaard L. Principles of cerebral perfusion imaging by bolus tracking. J Magn Reson Imaging 2005;22:710-7.
24. Kuwabara Y, Sasaki M, Hirakata H, Koga H, Nakagawa M, Chen T, et al. Cerebral blood flow and vasodilatory capacity in anemia secondary to chronic renal failure. Kidney Int 2002;61:564-9.
25. Borrelli M, Tamarozzi R, Colamussi P, Govoni M, Trotta F, Lappi S. Evaluation with MR, perfusion MR and cerebral flow SPECT in NPSLE patients. Radiol Med 2003;105:482-9.
26. Hochberg MC. Updating the American College of Rheumatology revised criteria for the classification of systemic lupus erythematosus. Arthritis Rheum 1997;40:1725.
27. Gladman D, Ginzler E, Goldsmith C, Fortin P, Liang M, Urowitz M, et al. The development and initial validation of the Systemic Lupus International Collaborating Clinics/American College of Rheumatology damage index for systemic lupus erythematosus. Arthritis Rheum 1996;39:363-9.
28. The American College of Rheumatology nomenclature and case definitions for neuropsychiatric lupus syndromes. Arthritis Rheum 1999;42:599-608.
29. Rempp KA, Brix G, Wenz F, Becker CR, Guckel F, Lorenz WJ. Quantification of regional cerebral blood flow and volume with dynamic susceptibility contrast-enhanced MR imaging. Radiology 1994;193:637-41.
30. Wu O, Ostergaard L, Weisskoff RM, Benner T, Rosen BR, Sorensen AG. Tracer arrival timing-insensitive technique for estimating flow in MR perfusion-weighted imaging using singular value decomposition with a block-circulant deconvolution matrix. Magn Reson Med 2003;50:164-74.
31. Magnotta VA, Bockholt HJ, Johnson HJ, Christensen GE, Andreasen NC. Subcortical, cerebellar, and magnetic resonance based consistent brain image registration. Neuroimage 2003;19:233-45.
32. Tanaka F, Vines D, Tsuchida T, Freedman M, Ichise M. Normal patterns on 99mTc-ECD brain SPECT scans in adults. J Nucl Med 2000;41:1456-64.
33. Speck O, Chang L, DeSilva NM, Ernst T. Perfusion MRI of the human brain with dynamic susceptibility contrast: gradient-echo versus spin-echo techniques. J Magn Reson Imaging 2000;12:381-7.
34. Wintermark M, Sesay M, Barbier E, Borbely K, Dillon WP, Eastwood JD, et al. Comparative overview of brain perfusion imaging techniques. J Neuroradiol 2005;32:294-314.
35. Lee PH, Joo US, Bang OY, Seo CH. Basal ganglia hyperperfusion in a patient with systemic lupus erythematosus-related parkinsonism. Neurology 2004;63:395-6.
36. Khubchandani RP, Viswanathan V, Desai J. Unusual neurologic manifestations (I): Parkinsonism in juvenile SLE. Lupus 2007;16:572-5.
37. Guadagno JV, Warburton EA, Jones PS, Fryer TD, Day DJ, Gillard JH, et al. The diffusion-weighted lesion in acute stroke: heterogeneous patterns of flow/metabolism uncoupling as assessed by quantitative positron emission tomography. Cerebrovasc Dis 2005;19:239-46.
38. Kim YS, Nur E, van Beers EJ, Truijen J, Davis SC, Biemond BJ, et al. Dynamic cerebral autoregulation in homozygous sickle cell disease. Stroke 2009;40:808-14.
39. Friberg L, Olsen TS. Cerebrovascular instability in a subset of patients with stroke and transient ischemic attack. Arch Neurol 1991;48:1026-31.
40. Sagiuchi T, Ishii K, Asano Y, Aoki Y, Kikuchi K, Jinguuji K, et al.

Interictal crossed cerebellar hyperperfusion on Tc-99m ECD SPECT. Ann Nucl Med 2001;15:369-72.
41. Cruz J, Nakayama P, Imamura JH, Rosenfeld KG, de Souza HS, Giorgetti GV. Cerebral extraction of oxygen and intracranial hypertension in severe, acute, pediatric brain trauma: preliminary novel management strategies. Neurosurgery 2002;50:774-9.
42. Moore DF, Altarescu G, Herscovitch P, Schiffmann R. Enzyme replacement reverses abnormal cerebrovascular responses in Fabry disease. BMC Neurol 2002;2:4.
43. Pollock JM, Deibler AR, Burdette JH, Kraft RA, Tan H, Evans AB, et al. Migraine associated cerebral hyperperfusion with arterial spin-labeled MR imaging. AJNR Am J Neuroradiol 2008;29:1494-7.
44. Ge Y, Law M, Johnson G, Herbert J, Babb JS, Mannon LJ, et al. Dynamic susceptibility contrast perfusion MR imaging of multiple sclerosis lesions: characterizing hemodynamic impairment and inflammatory activity. AJNR Am J Neuroradiol 2005;26:1539-47.
45. Hatazawa J, Shimosegawa E, Toyoshima H, Ardekani BA, Suzuki A, Okudera T, et al. Cerebral blood volume in acute brain infarction: A combined study with dynamic susceptibility contrast MRI and 99mTc-HMPAO-SPECT. Stroke 1999;30:800-6.
46. Smith M. Perioperative uses of transcranial perfusion monitoring. Neurosurg Clin N Am 2008;19:489-502, vii.
47. Sibbitt WL Jr, Sibbitt RR, Brooks WM. Neuroimaging in neuropsychiatric systemic lupus erythematosus. Arthritis Rheum 1999;42:2026-38.
48. Kikuchi K, Murase K, Miki H, Kikuchi T, Sugawara Y, Mochizuki T, et al. Measurement of cerebral hemodynamics with perfusion-weighted MR imaging: comparison with pre- and post-acetazolamide 133Xe-SPECT in occlusive carotid disease. AJNR Am J Neuroradiol 2001;22:248-54.
49. Kuo PH, Kanal E, Abu-Alfa AK, Cowper SE. Gadolinium-based MR contrast agents and nephrogenic systemic fibrosis. Radiology 2007;242:647-9.
50. Calamante F, Gadian DG, Connelly A. Quantification of perfusion using bolus tracking magnetic resonance imaging in stroke: assumptions, limitations, and potential implications for clinical use. Stroke 2002;33:1146-51.
51. Steup-Beekman G, Steens S, van Buchem M, Huizinga T. Anti-NMDA receptor autoantibodies in patients with systemic lupus erythematosus and their first-degree relatives. Lupus 2007;16:329-34.